J Parasit Dis (Oct-Dec 2022) 46(4):1011–1020
https://doi.org/10.1007/s12639-022-01520-3

ORIGINAL ARTICLE

Apoptotic changes in the intestinal epithelium of *Cryptosporidium*-infected mice after silver nanoparticles treatment versus nitazoxanide

Zeinab R. Hassan[1] · Doaa E. A. Salama[2] · Hanan F. Ibrahim[3]

Received: 21 May 2022 / Accepted: 29 June 2022 / Published online: 23 July 2022

Abstract *Cryptosporidium* has been identified as one of the prevalent opportunistic parasites that cause diarrhea, which may be persistent and fatal. Current chemotherapeutic agents, including nitazoxanide (NTZ), are frequently associated with therapeutic failure, and their roles in the induction of apoptosis in cryptosporidiosis remain to be a topic of debate. Thus, this study aimed to assess the apoptotic changes in cryptosporidiosis in immunocompetent (IC) and immunosuppressed (IS) mice after treatment with silver nanoparticles (AgNPs) and NTZ either alone or after loading. In total, 120 laboratory-bred Swiss albino mice were divided into two groups. Group A included IC mice, while Group B included IS mice. Both groups were divided into six subgroups: noninfected nontreated, infected nontreated, infected AgNP-treated, infected NTZ-treated, infected AgNP-loaded NTZ (full-dose)-treated, and infected AgNP-loaded NTZ (half-dose)-treated. The assessment was achieved through parasitological, histopathological, and apoptotic marker expression evaluation. AgNP-loaded NTZ (different doses) treatment showed the highest oocyst shedding reduction and remarkable improvement in histopathological changes, followed by individual treatment with NTZ and then AgNPs in IC and IS mice. Results of apoptotic marker expression revealed that AgNP-loaded NTZ treatment exhibited a promising role in regulating apoptotic changes in cryptosporidiosis through the expression of the lowest levels of cytochrome C and caspase-3 in IC and IS mice at the end of the experiment. Therefore, AgNP-loaded NTZ can be a potential therapeutic agent against cryptosporidiosis for IC and IS mice.

Keywords Apoptosis · Caspase3 · Cryptosporidiosis · Cytochrome C · Nitazoxanide · Silver nanoparticles

✉ Zeinab R. Hassan
zenabramadan.medg@azhar.edu.eg

[1] Department of Parasitology, Faculty of Medicine for Girls, Al-Azhar University, Cairo, Egypt

[2] Department of Pathology, Faculty of Medicine for Girls, Al-Azhar University, Cairo, Egypt

[3] Department of Microbiology and Immunology, Faculty of Medicine for Girls, Al-Azhar University, Cairo, Egypt

Introduction

Cryptosporidiosis is a severe gastrointestinal disease caused by Cryptosporidium spp. in humans and animals (Innes et al. 2020). Cryptosporidium has been identified as one of the most prevalent causes of diarrhea in children worldwide (Bones et al. 2019). This protozoan can be transmitted from one person to another by the fecal–oral route, through ingestion of contaminated food or drink, or through direct contact with infected cases and rarely via inhalation (Sponseller et al. 2014; Bauerfeind et al. 2016). In healthy individuals, cryptosporidiosis may cause acute watery diarrhea, nausea, vomiting, and fever (Dumaine et al. 2020). In humans, Cryptosporidium infection may lead to chronic joint pain, fatigue, and irritable bowel syndrome (Carter et al. 2019). The development of this parasite occurs inside the microvillus membrane of enterocytes, triggering villous atrophy and loss of villous enterocytes (Liu et al. 2014).

Nitazoxanide (NTZ) is the only approved chemotherapeutic agent for treating cryptosporidiosis in humans, but the drug has limited effects in immunocompromised patients. There are no available vaccinations for *Cryptosporidium parvum*, and oocysts are extremely resistant to

commonly used disinfectants (Innes et al. 2020). Silver nanoparticles (AgNPs) have received significant attention in recent years and are known to have many applications in various fields, including therapeutic potential against various infections (Khan et al. 2018).

AgNPs exhibit in vitro and in vivo antiparasitic activities against parasites, such as *Toxoplasma*, *Trypanosoma*, *Entamoeba histolytica*, *C. parvum*, *Leishmania*, and *Plasmodium* (Saad et al. 2015; Ahmed et al. 2017; Alajmi et al. 2019; Brito et al. 2020; Hassan et al. 2021).

Infection with microbial pathogens causes apoptosis or programmed cell death. Apoptosis is a defensive mechanism that controls host responses to invasive and noninvasive infections (Kapczuk et al. 2020). Cytochrome C (Cyto C) also plays a critical role in apoptosis. Activation of Bcl-2 family proapoptotic members or suppression of antiapoptotic members results in altered mitochondrial outer membrane permeability, leading to the release of Cyto C into the cytosol and activation of caspase-9, which then activates other caspases to accelerate apoptosis (Lee and Lee 2018).

Apoptosis has been reported in epithelial cells of small intestine villi in experimental *C. parvum* infections of multiple human cell lines and neonatal mice models (Sasahara et al. 2003). Caspase activation and Fas ligand-mediated apoptosis occur in *C. parvum* infections and are associated with a significant reduction in the number of intracellular parasites. In contrast, the *Cryptosporidium* parasite may actively upregulate survivin (Liu et al. 2008) or dysregulate microRNA expression (Wang et al. 2019) in infected human intestinal epithelial cells to suppress the apoptotic response to complete its endogenous developmental cycle.

The use of *Euphorbia prostrata* extract in the green synthesis of silver and titanium dioxide nanoparticles inhibited the in vitro growth of *Leishmania donovani*. This might be attributed to decreased reactive oxygen species (ROS) levels, which could then be responsible for the caspase-independent shift from apoptosis to massive necrosis (Zahir et al. 2015).

The anticancer potential of AgNPs generated from the dried stem section of *Eleutherococcus senticosus* has been postulated, which might be associated with ROS generation after caspase-3/p38 mitogen-activated protein kinase pathway activation to induce apoptosis in cancer colon (Kim et al. 2018).

This study aimed to assess the apoptotic effects of AgNPs alone and loaded NTZ versus NTZ alone in mice infected with *Cryptosporidium*.

Material and method

Parasite

Stool samples were collected from the outpatient clinic of Alzhara Hospital, transferred to the Parasitology Department of the Theodor Bilharz Research Institute (TBRI), and microscopically screened by Kinyoun's acid-fast stain (cold method) to determine the presence of *Cryptosporidium* oocysts. For preparation of *Cryptosporidium* oocysts inoculum according to. Abdou et al. (2013) and Hassan et al. (2021), the positive samples were sieved and centrifuged at 500 × g for 5 min, the supernatant fluid were removed. The sediment was washed twice in phosphate-buffer saline (PBS), centrifuged at 13,000 × g for 2 min. Fecal materials were removed after repeated washing and centrifugation then the number of *Cryptosporidium* oocysts in the given inoculum were counted to prepare the infecting dose for each mouse.

Treatment regimen

Treatment started at the 10th day post-infection (dpi) for 3 consecutive days only. AgNPs solution (Nano tech Egypt Company, Cairo, Egypt) was given orally by orogastric gavage at a dose of 5 mg/kg/mouse/day (Said et al. 2012; Hassan et al. 2021). NTZ suspension (Utopia; Cairo/Egypt) was given orally by orogastric gavage at a dose of 100 mg/kg/mouse/day or at a half-dose (50 mg/kg/mouse/day) (Abd El-Aziz et al. 2014; Shaaban et al. 2021). For AgNPs Loaded NTZ, AgNPs (5 mg/kg) and NTZ (100 mg/kg or 50 mg/kg) were vortexed together for 1 h in a closed container to load AgNPs with NTZ, and then the mixed solutions were given orally.

Experimental animals

In total, 120 Laboratory-bred Swiss albino mice weighing 20–25 g and aged 3 to 5 weeks were housed in standard laboratory conditions with free access to water and diet containing 24% protein, 4% fat and about 4 to 5% fiber. Mice were provided by TBRI Animal Producing Unit. Mice free of any parasites were selected. Mice were then divided into immunocompetent (IC) and immunosuppressed (IS) groups. Immune suppression of mice was performed by using dexamethasone (Dexazone 0.5 mg) (Kahira Pharmaceuticals and Chemical Industries Company, Cairo, Egypt) after dissolving the tablet in distilled water and given orally by orogastric gavage at a dose of 0.25 mg/g/day for 14 successive days before inoculation with *Cryptosporidium* oocysts (Abdou et al. 2013). Each mouse was infected by oral inoculation with isolated

Cryptosporidium oocysts in a dose of ~ 10^4 oocysts/-mouse (Hassan et al. 2021; Moawad et al. 2021). Mice were sacrificed using intraperitoneal anesthesia on 28th dpi. Parasitological, histopathological and apoptotic markers expression parameters were used to assess the study objective.

Experimental mice groups

The 120 mice were divided into two main groups.

Group A: IC mice (n = 60) were divided into six sub-groups (SGs).

- SGA1: noninfected IC (n = 10).
- SGA2: infected nontreated IC (n = 10).
- SGA3: infected IC receiving AgNPs (n = 10).
- SGA4: infected IC receiving NTZ (n = 10).
- SGA5: infected IC receiving AgNP-loaded NTZ (full-dose; n = 10).
- SGA6: infected IC receiving AgNP-loaded NTZ (half-dose; n = 10).

Group B: IS mice (n = 60) were divided into six SGs.

- SGB1: noninfected nontreated IS (n = 10).
- SGB2: infected nontreated IS (n = 10).
- SGB3: infected IS receiving AgNPs (n = 10).
- SGB4: infected IS receiving NTZ (n = 10).
- SGB5: infected IS receiving AgNP-loaded NTZ (full-dose; n = 10).
- SGB6: infected IS receiving AgNP-loaded NTZ (half-dose; n = 10).

Parasitological assessment

Daily examination of fecal pellet after inoculation with *Cryptosporidium* oocysts was performed to determine the peak of oocyst shedding to start treatment. After treatment administration, fecal pellets were collected from all infected mice SGs at 14th and 28th dpi and subjected to microscopical examination using the Kinyoun's Acid-Fast stain (cold method) to count the number of *Cryptosporidium* oocysts (Garcia 2007; Hassan et al. 2021).

Histopathological assessment

About 1-cm-long segments from upper part of the small intestine were cut off and fixed in 10% formalin, and processed for paraffin embedding sections, and 4-µm-thick sections were stained with hematoxylin & eosin stain (H&E) according to Ross and Pawlina (2016).

Apoptotic markers expression assessment

Quantitative measurement of Cyto C by enzyme-linked immunosorbent assay (ELISA) in tissue lysates

Cyto C level was assessed in tissue lysates of homogenized parts of small intestinal tissue. Parts of small intestine were sliced and washed well in PBS to eliminate blood. The samples were centrifuged at 18,000 × g for 20 min, and the supernatant was collected and kept at − 70 °C for further usage of an ELISA kit (ab210575; Sigma; USA) to evaluate Cyto C levels.

The steps of protocol were as follows. First, 50 µl of samples or standards were added to the wells, followed by 50 µl of the antibody mix, and incubated for 1 h at room temperature with shaking. The wells were washed thrice with wash buffer to remove unbound material. TMB substrate (100 µl) was added and incubated for 10 min in the dark with shaking. The reaction was stopped by addition 100 µl of Stop Solution. Optical density was measured at 450 nm, and the levels were calculated according to standard curve of the manufacturer's instructions.

Caspase 3 immunohistochemistry

Immunohistochemical staining was performed on paraffin-embedded sections with a thickness of 4 µm. Polyclonal rabbit anti-active caspase-3 was uses as primary antibody and biotinylated goat anti-rabbit antibody as secondary antibody (DAKO, Carpinteria, California, USA). For each assessment, standard positive and negative control sections were used. Each section's represented fields were chosen randomly and interpreted in a blinded way, considering the stained cytoplasm of intestinal epithelium as positive for caspase 3 expression. After estimating the intensity of staining and the proportion of positive cells, caspase 3 expression in intestinal tissue was assessed using the H score as follows: −, negative; +, mild staining; ++, moderate staining; and +++, strong staining (−): negative, (+):mild staining, (++): moderate staining, (+++): strong staining (El-Kady et al. 2021; Samaka et al. 2021).

Statistical analysis

Data were collected, tabulated and analyzed by using Statistical Package for the Social Sciences version 20. Descriptive statistics; means and standard deviation (SD). Student's *t*-test and analysis of variance were used. Significant was considered at P value < 0.05*.

Result

Parasitological results

The peak of Cryptosporidium oocyst shedding was on the 10th dpi in Groups A and B, with a significant reduction in oocyst shedding in both groups after treatment on different days (14th and 28th days) and the highest reduction after treatment with AgNP-loaded NTZ (different doses) in SGA5, SGA6, SGB5, and SGB6 (Tables 1, 2). A significant reduction in oocyst shedding was noted after treatment in Group A compared to Group B on the 28th dpi, except for SGs treated with AgNPs (SGA3 and SGB3; Table 3). There was a significant oocyst shedding reduction in SGA3, SGA5, and SGA6 compared to NTZ-treated SGA4 on different days post-infection (Table 4). SGB3 and SGB6 showed a significant reduction compared to NTZ-treated SGB4 only on the 28th dpi, whereas AgNP-loaded NTZ (full-dose)-treated SGB5 showed a significant reduction on different days post-infection (Table 5).

Histopathological results

Sections of the small intestine in the noninfected IC (SGA1) showed normal villous architecture (Fig. 1a) and mild inflammation and edema in noninfected IS (SGB1; Fig. 1b). Meanwhile, infected nontreated SGA2 and SGB2 showed severe pathological changes (Fig. 1c, d, respectively).

Histopathological examination of various IC and IS SGs showed varying degrees of improvement after treatment (Fig. 1e–l). SGA5 and SGB5 [infected AgNPs + NTZ (full-dose)-treated IC and IS] displayed a remarkable improvement in histopathological changes (Fig. 1i, j), respectively, followed by SGA6 and SGB6 [infected AgNPs + NTZ (half-dose)-treated IC and IS; Fig. 1k, l], respectively.

Table 1 The mean count of *Cryptosporidium oocysts* in Groups A on the 14th, and 28th days post infection (dpi)

Group A	14th dpi	28th dpi
SGA2	34,400 ± 4996	551 ± 96
SGA3	13,733 ± 3885	247 ± 94.4
SGA4	8333 ± 1528	49 ± 29.2
SGA5	2267 ± 1087	0
SGA6	4517 ± 956	3 ± 1.5
ANOVA		
F sample	56.2	43.96
P value	0.000*	0.000*

A2: infected non-treated IC, A3: infected IC receiving AgNP, A4: infected IC receiving NTZ, A5: infected IC receiving AgNPs-loaded NTZ (full dose), A6: infected IC receiving AgNPs-loaded NTZ (½ dose)

Significant: $P < 0.05$*

Table 2 The mean count of *Cryptosporidium oocysts* in Groups B on the 14th, and 28th days post infection (dpi)

Group B	14th dpi	28th dpi
SGB2	55,851 ± 11,900	873 ± 88
SGB3	18,322 ± 5489	346 ± 98.5
SGB4	11,622 ± 6710	210 ± 60.2
SGB5	3839 ± 1586	14.3 ± 9.3
SGB6	6147 ± 1652	77.3 ± 11.6
ANOVA		
F sample	30.5	82.7
P value	0.000*	0.000*

B2: infected non-treated IS, B3: infected IS receiving AgNP, B4: infected IS receiving NTZ, B5: infected IS receiving AgNPs-loaded NTZ (full dose), B6: infected IS receiving AgNPs-loaded NTZ (½ dose)

Significant: $P < 0.05$*

Apoptotic marker results

Cyto C release assay

Results revealed a significantly higher level of Cyto C (ng/mg) in all infected nontreated IC and IS mice SGs (SGA2 and SGB2) than noninfected SGs (SGA1 and SGB1), with a significant difference in all infected treated SGs of IS mice in Group B compared to all infected treated SGs of IC mice in Group A (Table 6). NTZ-treated mice exhibited significantly higher levels of Cyto C (SGA4 of IC and SGB4 of IS) than AgNPs-loaded NTZ (different doses)-treated mice SGA5 and SG6 and SGB5 and SGB6, respectively (Table 7).

Caspase 3 apoptotic activity

Immunohistochemistry results showed negative apoptotic expression of caspase-3 in SGA1 (noninfected nontreated IC; Fig. 2a), whereas SGA1 (noninfected non treated IS) showed mild apoptotic expression of caspase-3 (Fig. 2b). In contrast, SGA2 and B2 (infected non treated IC & IS respectively) showed strong expression of caspase-3 apoptotic activity (Fig. 2c, d). Intestinal sections of all infected treated IC and IS SGs showed a decreased peak of caspase-3 expression with varying score (Fig. 2e–l). In contrast, SG5 treated with AgNPs-loaded NTZ (full dose) showed no apoptotic expression of caspase-3 (Fig. 2i).

Table 3 Comparison between mean count of *Cryptosporidium oocysts* in SGS of Groups A and B on the 14th, and 28th days post infection (dpi)

SGS	14th dpi		28th dpi	
	T. test	*P* value	T. test	*P* value
SGA2 SGB2	4.017	$P < 0.01$*	6.057	$P < 0.001$*
SGA3 SGB3	1.672	$P > 0.05$	1.777	$P > 0.05$
SGA4 SGB4	1.171	$P > 0.05$	5.894	$P < 0.001$*
SGA5 SGB5	2.003	$P > 0.05$	3.767	$P < 0.01$*
SGA6 SGB6	2.092	$P > 0.05$	15.56	$P < 0.001$*

A2: infected nontreated IC, A3: infected IC receiving AgNP, A4: infected IC receiving NTZ, A5: infected IC receiving AgNPs loaded NTZ (full dose), A6: infected IC receiving AgNPs loaded NTZ (½ dose). B2: infected non-treated IS, B3: infected IS receiving AgNP, B4: infected IS receiving NTZ, B5: infected IS receiving AgNPs-loaded NTZ (full dose), B6: infected IS receiving AgNPs-loaded NTZ (½ dose)

Significant: $P < 0.05$*

Table 4 Mean count of *Cryptosporidium oocysts* in SGA 4 versus SGA (3, 5, and 6) on the 14th, and 28th days post infection (dpi)

SGS	14th dpi		28th dpi	
	T. test	*P* value	T. test	*P* value
SGA4 SGA3	3.168	$P < 0.01$*	4.908	$P < 0.01$*
SGA4 SGA5	7.924	$P < 0.001$*	4.11	$P < 0.01$*
SGA4 SGA6	5.186	$P < 0.001$*	3.854	$P < 0.01$*

A3: infected IC receiving AgNP, A4: infected IC receiving NTZ, A5: infected IC receiving AgNPs loaded NTZ (full dose), A6: infected IC receiving AgNPs loaded NTZ (½ dose)

Significant: $P < 0.05$*

Table 5 Mean count of *Cryptosporidium oocysts* in SGB 4 versus SGB (3, 5, and 6) on the 14th, and 28th days post infection (dpi)

SGS	14th dpi		28th dpi	
	T. test	*P* value	T. test	*P* value
SGB4 SGB3	1.893	$P > 0.05$	2.886	$P < 0.05$*
SGB4 SGB5	2.765	$P < 0.05$*	7.870	$P < 0.001$*
SGB4 SGB6	1.941	$P > 0.05$	5.302	$P < 0.001$*

B3: infected IS receiving AgNP, B4: infected IS receiving NTZ, B5: infected IS receiving AgNPs-loaded NTZ (full dose), B6: infected IS receiving AgNPs-loaded NTZ (½ dose)

Significant: $P < 0.05$*

Discussion

In this study, the intensity of *Cryptosporidium* oocyst shedding was noted to be higher in IS than IC mice. This finding was consistent with that of Abdou et al. (2013), Aly et al. (2017) and Moawad et al. (2021) who reported a higher *Cryptosporidium* parasitic load in groups with an immunosuppression state.

NTZ treatment significantly reduced oocyst shedding in IC and IS mice. Still, there was a significant difference between the mean counts of oocyst shedding in both groups, being lower in IC than IS mice after NTZ treatment. These results were consistent with that of Abdou et al. (2013) and Moawad et al. (2021), who demonstrated that IC mice treated with NTZ showed significant lower mean counts than IS ones, with regard to the levels of fecal oocyst shedding and internal developmental stages of the *Cryptosporidium* in both. In contrast, AgNP treatment revealed a significant reduction in oocyst shedding in IC and IS mice and relatively no significant difference in the mean count of oocyst shedding in both groups. Results suggested that AgNPs exert their effects independent of the immune response in contrast to NTZ. Similarly, the effectiveness of AgNPs as a water disinfectant was established by their capacity to significantly reduce the number and viability of *C. parvum* oocysts (Hassan et al. 2019). Also, in vivo anti-*Cryptosporidium* effect of AgNPs independent on the immunostate of experimentally infected mice has been reported (Hassan et al. 2021). This can be clarified by Xu et al. (2013), who stated that AgNPs have significant adjuvant action and may trigger both Th1 and Th2 immune responses and boost cytokine levels that can play a role in controlling the infection.

Furthermore, in this study, AgNPs-loaded NTZ treatment exhibited potent anti-*Cryptosporidium* effects with highest oocyst shedding reduction. This synergistic action between AgNPs and NTZ agreed with the findings of Hassan et al. (2021), who reported that loading of different doses of NTZ (200 and 100 mg/kg) on AgNPs, increased their efficacy and significantly reduced *Cryptosporidium* oocyst shedding. This may be explained by Khalil et al. (2013), who demonstrated that nanoparticles could serve as drug carriers, increasing bioavailability, modifying pharmacokinetics, and reducing adverse effects when released into target tissues. These were in accordance with Sedighi et al. (2016), who reported that NTZ loaded on solid lipid nanoparticles treatment in neonatal rats showed more

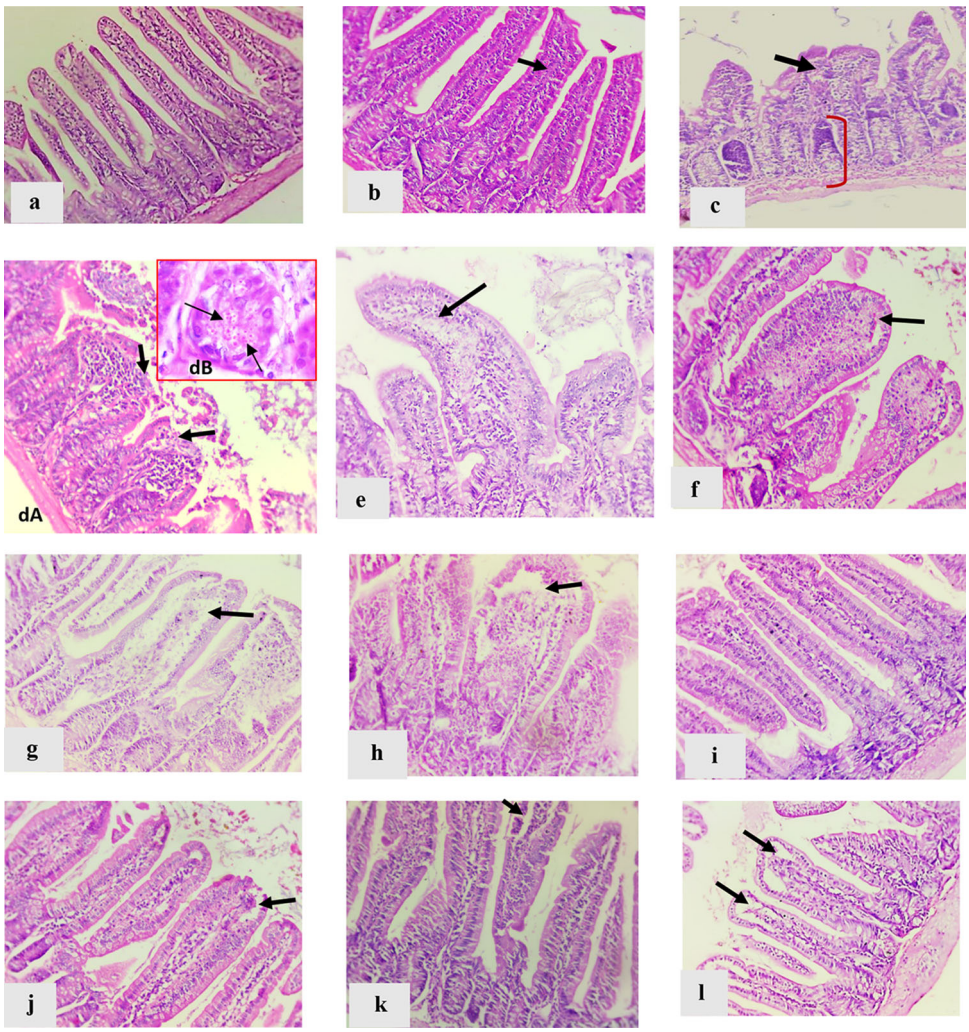

Fig. 1 Sections of the small intestine of mice stained with H&E. **a** SGA1 (noninfected IC) with normal intestinal villous architecture (×200). **b** SGB1 (noninfected IS) with mild villous edema (arrow) with mild cellular infiltration. **c** SGA2 (infected nontreated IC) with severe villous atrophy with expansion of villous core by excess inflammatory cellular infiltrate (arrow) and crypt hyperplasia (red line; ×200). **d** SGB2 (infected nontreated IS) with marked villous shortening an expanded villous core by excess inflammatory cellular infiltrate with superficial ulceration (arrows; ×200; dA) and *Cryptosporidium* oocysts (arrows; ×1000; dB). **e** SGA3 (infected AgNPs-treated IC) with moderate villous shortening with an expanded villous core by edema and moderate inflammatory cellular infiltrate (arrow; ×200). **f** SGB3 (infected AgNPs treated IS) with moderate villous shortening an expanded villous core by edema and moderate inflammatory cellular infiltrate (arrow; ×200). **g** SGA4 (infected NTZ-treated IC) with moderate villous shortening and blunting with an expanded villous core by edema and moderate inflammatory cellular infiltrate (arrow; ×200). **h** SGB4 (infected NTZ-treated IS) with moderate to severe villous shortening and blunting with an expanded villous core by edema and moderate inflammatory cellular infiltrate (arrow; ×200). **i** SGA5 [infected AgNPs + NTZ (full-dose)-treated IC] with near normal villous architecture with mild cellular infiltration (×200). **j** SGB5 [infected AgNPs + NTZ (full-dose)-treated IS] showing mild villous atrophy with mild edema and cellular infiltration (arrow; ×200). **k** SGA6 (infected AgNPs + NTZ (½ dose) treated IC) with mild villous atrophy with mild edema and cellular infiltration (arrow; ×200). **l** SGB6 [infected AgNPs + NTZ (half-dose)-treated IS] showing mild villous atrophy with mild edema and cellular infiltration (arrow; ×200)

effectiveness against *Cryptosporidium* infection than the free drug. Also, Moawad et al. (2021) noticed that mice received NTZ loaded CS treatment showed obvious reduction in *Cryptosporidium* oocysts. Similarly, NTZ loaded on AgNPs exhibited the highest effectiveness against animal model of chronic toxoplasmosis, attained by the synergistic action (Mohammed et al. 2021).

Histopathological examination of the intestinal sections of the infected non treated IC and IS mice showed sever destructive effects on the structure of the intestinal mucosa as result of infection with *Cryptosporidium* oocysts, that were more severe in IS mice than IC ones (Liu et al. 2014; Taha et al. 2017; Oshiba et al. 2018; Abdelhamed et al. 2019; Hassan et al. 2021; Moawad et al. 2021).

Table 6 The mean level of Cytochrome C (ng/mg) in Groups A and B

Group A	Mean ± SD	Group B	Mean ± SD	T. test *P* value
SGA1	51.1 ± 0.42	SGB1	67.2 ± 1.27	17.02
				$P < 0.01$*
SGA2	124.75 ± 6.15	SGB2	110.95 ± 1.91	3.03
				$P > 0.05$
SGA3	117.05 ± 0.21	SGB3	105.7 ± 0.57	26.42
				$P < 0.01$*
SGA4	96.3 ± 0.57	SGB4	90.17 ± 0.89	8.20
				$P < 0.05$*
SGA5	79.7 ± 0.57	SGB5	71.35 ± 1.48	7.45
				$P < 0.05$*
SGA6	82.6 ± 0.71	SGB6	77.6 ± 0.71	7.04
				$P < 0.05$*
ANOVA		ANOVA		
F sample	222.32	*F* sample	497.1	
P value	0.000*	*P* value	0.000*	

A1: noninfected nontreated IC. A2: infected nontreated IC, A3: infected IC receiving AgNP, A4: infected IC receiving NTZ, A5: infected IC receiving AgNPs loaded NTZ, A6: infected IC receiving AgNPs loaded NTZ (½ dose). B1: noninfected non-treated IS, B2: infected non-treated IS, B3: infected IS receiving AgNP, B4: infected IS receiving NTZ, B5: infected IS receiving AgNPs loaded NTZ, B6: infected IS receiving AgNPs loaded NTZ (½ dose)

Significant: $P < 0.05$*

Table 7 The mean level of Cytochrome C in Groups A4 and B4 versus SGA (3, 5, 6) and SGB (3, 5, 6) respectively

Group A	T. test *P* value	Group B	T. test P value
SGA4	48.31	SGB4	20.78
SGA3	$P < 0.001$*	SGB3	$P < 0.01$*
SGA4	29.12	SGB4	15.411
SGA5	$P < 0.01$*	SGB5	$P < 0.01$*
SGA4	21.279	SGB4	15.614
SGA6	$P < 0.01$*	SGB6	$P < 0.01$*

A3: infected IC receiving AgNP, A4: infected IC receiving NTZ, A5: infected IC receiving AgNPs loaded NTZ, A6: infected IC receiving AgNPs loaded NTZ (½ dose). B3: infected IS receiving AgNP, B4: infected IS receiving NTZ, B5: infected IS receiving AgNPs-loaded NTZ, B6: infected IS receiving AgNPs-loaded NTZ (½ dose)

Significant: $P < 0.05$*

Treatment with NTZ has also helped partially improve histopathological changes in both IC and IS mice, a finding consistent with that of Moawad et al. (2021) and Oshiba et al. (2018), who reported moderate histopathological changes after receiving NTZ in *Cryptosporidium*-infected mice. Current histopathological results of AgNPs were nearly similar to Hassan et al. (2021), who found that AgNPs treatment showed a partial improvement in the histopathological changes in IC and IS mice. In contrast, AgNPs-loaded NTZ treatment revealed a marked improvement in histopathological changes after *Cryptosporidium* infection. These findings agreed with Abdelhamed et al. (2019), Hassan et al. (2021) and Moawad et al. (2021), who noticed improvement of the intestinal histopathological changes in *Cryptosporidium*-infected mice after treatment of NTZ loaded on nanoparticles.

Apoptotic assay of Cyto C concentrations in intestinal tissue extracts showed a significant increase in infected nontreated IC and IS mice with higher levels in IC than IS mice. Treatment with AgNPs-loaded NTZ (different doses) in IC and IS mice exerted the lowest level of Cyto C release among infected treated mice SGs, followed by individual treatment with NTZ, and then AgNPs. Liu et al. (2009) explained the essential role of apoptosis against cryptosporidiosis and the in vitro biphasic modulation to control the infection by either Bcl-2 activation or decreasing apoptosis by the pan-caspase inhibitor. Activation of pro apoptotic members resulted in Cyto C release into the cytosol, activating other caspases to accelerates apoptosis (Lee and Lee 2018).

Similarly, immunohistochemical results of caspase-3 apoptotic activity expression in intestinal sections, revealed negative expression in noninfected IC mice. In contrast, noninfected IS ones showed mild expression, which may

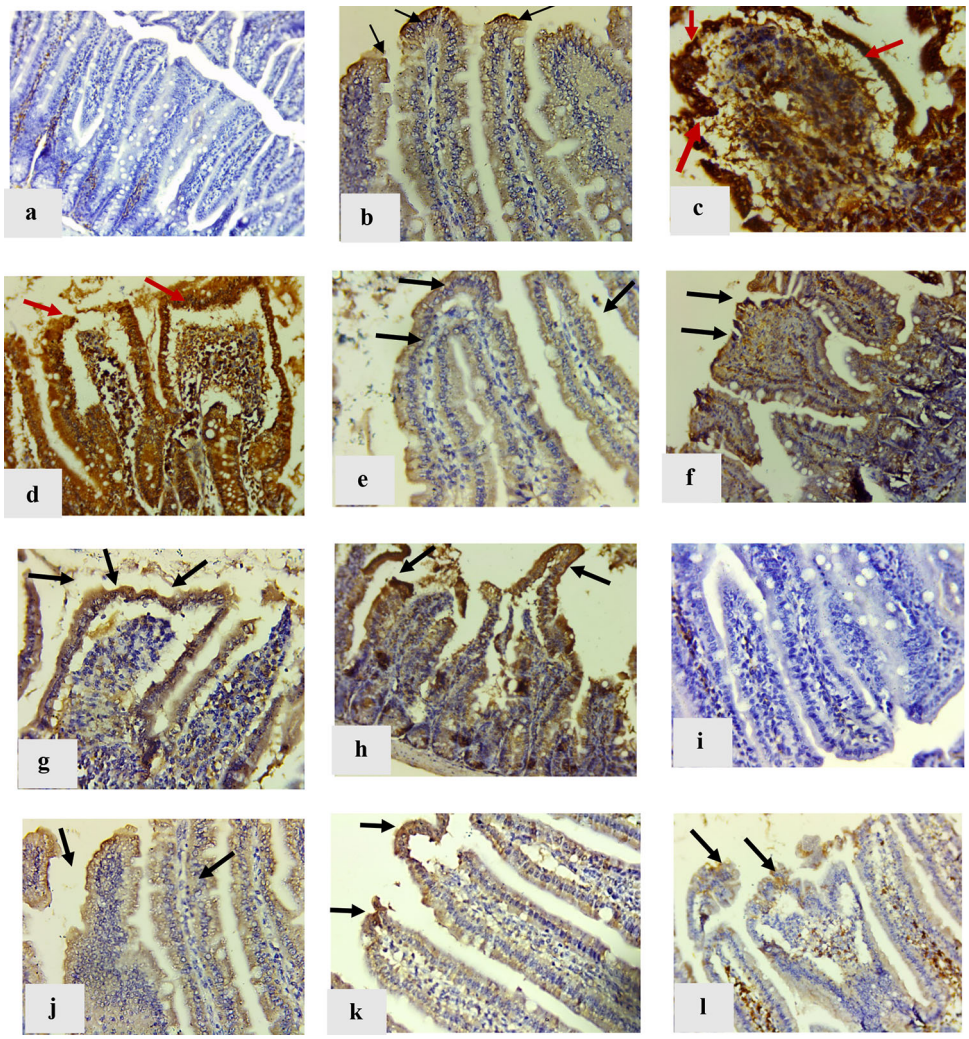

Fig. 2 Photomicrograph of the intestinal sections of mice (Immunohistochemical staining for Caspase 3). **a** SGA1 (noninfected IC) with negative expression (−; ×200). **b** SGB1 (noninfected IS) with brown cytoplasmic staining in intestinal epithelium, mild expression (+; arrows; ×400). **c** SGA2 (infected nontreated IC) with strong expression (+++; arrows; ×400). **d** SGB2 (infected nontreated IS) with strong expression (+++; arrows; ×400). **e** SGA3 (infected AgNPs-treated IC) with moderate expression (++; arrows; ×400). **f** SGB3 (infected AgNPs-treated IS) with moderate expression (++; arrows; ×200). **g** SGA4 (infected NTZ-treated IC) with moderate expression (++; arrows; ×400). **h** SGB4 (infected NTZ-treated IS) with moderate expression (++; arrows; ×200). **i** SGA5 [infected AgNPs + NTZ (full-dose)-treated IC] with negative expression (−; ×200). **j** SGB5 [infected AgNPs + NTZ (full-dose)-treated IS] with mild expression (+; arrows; ×200). **k** SGA6 [infected AgNPs + NTZ (half-dose)-treated IC] (infected AgNPs + NTZ (½ dose) treated IC) with mild expression (+; arrows; ×200). **l** SGB6 [infected AgNPs + NTZ (half-dose)-treated IS] with mild expression (+; arrows; ×200)

be due to effect of dexamethasone administration. This agreed with the findings of Liu et al. (2016), who noticed a slight expression of caspase-3 in uninfected malnourished mice, as immunosuppression can arise after malnutrition state. This was also consistent with the findings of Samaka et al. (2021), who reported mild caspase-3 apoptotic expression in noninfected IS mice. In contrast, strong expression in infected nontreated IC and IS mice agreed with previous observations (Sasahara et al. 2003; Liu et al. 2008; Samaka et al. 2021). AgNPs-loaded NTZ (full-dose) treatment in IC and IS mice SGs showed negative expression, which may be due to the clearing of the infection documented by no cyst shedding at time of scarification and near normal villous architecture in the histopathological results. Although, AgNPs-loaded NTZ (half-dose) treatment in IC and IS mice SGs showed mild caspase-3 apoptotic expression, these results were better than individual treatment with either NTZ or AgNPs, which revealed moderate expression of caspase-3. All infected IC mice showed higher level of Cyto C release and caspase-3 expression than corresponded infected IS mice, a finding consistent with that of Samaka et al. (2021).

Apoptosis of infected epithelial cells assists the infected host in limiting the spread of the infection and helps in parasite clearance (Uchiyama and Tsutsui 2015; Liu et al. 2016). Samaka et al. (2021) reported that the NTZ treatment induced apoptosis in infected intestinal cells through caspase-3 expression. Also, AgNPs showed apoptotic caspase-dependent apoptosis against infected cell (Zahir et al. 2015; Kim et al. 2018). This may explain the highest anti-*Cryptosporidium* efficacy of AgNPs loaded NTZ versus NTZ alone or AgNPs individually as a result of caspase-3 upregulation in infected intestinal cells that accelerate the clearance of infection.

Conclusion

This is the first study on the apoptotic changes in cryptosporidiosis after AgNPs treatment. As per the findings of this study, AgNPs-loaded NTZ elucidated a significant anti-*Cryptosporidium* potential on parasitological, histopathological and apoptotic markers expression assessment. Hence, it is proven that NTZ has increased therapeutic potential against cryptosporidiosis when loaded on AgNPs.

Author's contribution ZRH designed methodology, performed assessment parameters and wrote the manuscript. DEAS performed the histopathological and immunohistochemical assessment. HFI contributed in the assessment of the parameters and revised the manuscript. All authors have read and agreed to the initial draft.

Funding All authors declare that they have no financial interests and no funds, grants, or other support received.

Data availability All data generated or analyzed during this study are included in this published article.

Declarations

Conflict of interest All authors declare no conflict of interest.

Ethical approval This study work was performed in accordance to the Ethics Committee of the Faculty of Medicine for Girls Al-Azhar University and TBRI and the valid international guidelines for animal handling. The Protocol was approved by the Ethics Committee of Faculty of Medicine for Girls Al-Azhar University (RHDIRB/2018122001, Protocol No. 564/2021).

References

Abd El-Aziz TM, El-Beih NM, Soufy H, Naser S, Khalil FAM (2014) Effect of Egyptian propolis on lipid profile and oxidative status in comparison with nitazoxanide in immunosuppressed rats infected with *Cryptosporidium* spp. Glob Vet 13(1):17–27. https://doi.org/10.1016/j.apjtm.2017.03.004

Abdelhamed EF, Fawzy EM, Ahmed SM, Zalat RS, Rashed HE (2019) Effect of nitazoxanide, artesunate loaded polymeric nano fiber and their combination on experimental cryptosporidiosis. Iran J Parasitol 14(2):240–249

Abdou AG, Harba NM, Afifi AF, Elnaidany NF (2013) Assessment of *Cryptosporidium parvum* infection in immunocompetent and immunocompromised mice and its role in triggering intestinal dysplasia. Int J Infect Dis 17:593–600. https://doi.org/10.1016/j.ijid.2012.11.023

Ahmed ZA, Mustafa TA, Ardalan NM, Idan EM (2017) In vitro toxicity evaluation of silver nanoparticles on *Entamoeba histolytica* trophozoite. Baghdad Sci J 14:509–515. https://doi.org/10.21123/bsj.2017.14.3.0509

Alajmi RA, Al-Megrin WA, Metwally D, Al-Subaie H, Altamrah N, Barakat AM, Abdel Moneim AE, Al-Otaibi TT, El-Khadragy M (2019) Anti-*Toxoplasma* activity of silver nanoparticles green synthesized with *Phoenix dactylifera* and *Ziziphus spina-christi* extracts which inhibits inflammation through liver regulation of cytokines in Balb/c mice. Biosci Rep 39(5):BSR20190379. https://doi.org/10.1042/BSR20190379

Aly NSM, Selem RF, Zalat RS, Khalil H, Hussien BE (2017) An innovative repurposing of mefloquine; assessment of its therapeutic efficacy in treating *Cryptosporidium* infection in both immunocompetent and immunocompromised mice. J Egypt Soc Parasitol 47(2):253–262

Bauerfeind R, Von Graevenitz A, Kimmig P, Schiefer HG, Schwarz TF, Slenczka W, Zahner H (2016) Zoonoses: infectious diseases transmissible between animals and humans, 4th edn. ASM Press, Washington, DC

Bones AJ, Jossé L, More C, Miller CN, Michaelis M, Tsaousis AD (2019) Past and future trends of *Cryptosporidium* in vitro research. Exp Parasitol 196:28–37. https://doi.org/10.1016/j.exppara.2018.12.001

Brito TK, Silva Viana RL, Gonçalves Moreno CJ, da Silva BJ, de Sousa L, Júnior F, Campos de Medeiros MJ, Melo-Silveira RF, Almeida-Lima J, de Lima PD, Sousa Silva M, Oliveira Rocha HA (2020) Synthesis of silver nanoparticle employing corn cob xylan as a reducing agent with anti-*Trypanosoma cruzi* activity. Int J Nanomed 15:965–979. https://doi.org/10.2147/IJN.S216386

Carter BL, Stiff RE, Elwin K et al (2019) Health sequelae of human cryptosporidiosis—a 12-month prospective follow-up study. Eur J Clin Microbiol Infect Dis 38:1709–1717. https://doi.org/10.1007/s10096-019-03603-1

Dumaine JE, Tandel J, Striepen B (2020) *Cryptosporidium parvum*. Trends Parasitol 36(5):485–486. https://doi.org/10.1016/j.pt.2019.11.003

El-Kady AM, Abdel-Rahman IAM, Fouad SS, Allemailem KS, Istivan T, Ahmed SFM, Hasan AS, Osman HA, Elshabrawy HA (2021) Pomegranate peel extract is a potential alternative therapeutic for giardiasis. Antibiotics (Basel) 10(6):705. https://doi.org/10.3390/antibiotics10060705

Garcia LS (2007) Intestinal protozoa: flagellates and ciliates. Diagnostic medical parasitology, part II, 5th edn. ASM Press, Washington, DC, pp 771–812

Hassan D, Farghali M, Eldeek H, Gaber M, Elossily N, Ismail T (2019) Antiprotozoal activity of silver nanoparticles against *Cryptosporidium parvum* oocysts: new insights on their feasibility as a water disinfectant. J Microbiol Methods 165:105698. https://doi.org/10.1016/j.mimet.2019.105698

Hassan ZR, Hussein FO, Rabia IS, Abd Rabbo MA (2021) Effect of silver nanoparticles loaded nitazoxanide in the treatment of murine cryptosporidiosis in immunocompetent and immunosuppressed mice. Al-Azhar Univ J Virus Res Stud 3(1):1–15. https://doi.org/10.1007/s12639-020-01337-y

Innes EA, Chalmers RM, Wells B, Pawlowic MC (2020) A one health approach to tackle cryptosporidiosis. Trends Parasitol 36:290–303. https://doi.org/10.1016/j.pt.2019.12.01

Kapczuk P, Kosik-Bogacka D, Kupnicka P, Metryka E, Simińska D, Rogulska K, Skórka M, Gutowska I, Chlubek D, Baranowska-Bosiacka I (2020) The influence of selected gastrointestinal parasites on apoptosis in intestinal epithelial cells. Biomolecules 10(5):674. https://doi.org/10.3390/biom10050674

Khalil NM, de Mattos AC, Carraro TC, Ludwig DB, Mainardes RM (2013) Nanotechnological strategies for the treatment of neglected diseases. Curr Pharm Des 19:7316–7329. https://doi.org/10.2174/13816128194131219135458

Khan SU, Saleh TA, Wahab A, Khan MH, Khan D, Khan WU, Rahim A, Kamal S, Khan FU, Fahad S (2018) Nanosilver: new ageless and versatile biomedical therapeutic scaffold. Int J Nanomed 13:733–762. https://doi.org/10.2147/IJN.S153167

Kim CG, Castro-Aceituno V, Abbai R, Lee HA, Simu SY, Han Y, Hurh J, Kim YJ, Yang DC (2018) Caspase-3/MAPK pathways as main regulators of the apoptotic effect of the phyto-mediated synthesized silver nanoparticle from dried stem of *Eleutherococcus senticosus* in human cancer cells. Biomed Pharmacother 99:128–133. https://doi.org/10.1016/j.biopha.2018.01.050

Lee YJ, Lee C (2018) Porcine delta corona virus induces caspase-dependent apoptosis through activation of the cytochrome c-mediated intrinsic mitochondrial pathway. Virus Res 253:112–123

Liu J, Enomoto S, Lancto CA, Abrahamsen MS, Rutherford MS (2008) Inhibition of apoptosis in *Cryptosporidium parvum*-infected intestinal epithelial cells is dependent on survivin. Infect Immun 76:3784–3792. https://doi.org/10.1128/IAI.00308-08

Liu J, Deng M, Lancto CA, Abrahamsen MS, Rutherford MS, Enomoto S (2009) Biphasic modulation of apoptotic pathways in *Cryptosporidium parvum*-infected human intestinal epithelial cells. Infect Immun 77:837–849. https://doi.org/10.1128/IAI.00955-08

Liu H, Shen Y, Yin J, Yuan Z, Jiang Y, Xu Y, Pan W, Hu Y, Cao J (2014) Prevalence and genetic characterization of *Cryptosporidium, Enterocytozoon, Giardia and Cyclospora* in diarrheal outpatients in China. BMC Infect Dis 14(1):290–292. https://doi.org/10.1186/1471-2334-14-25

Liu J, Bolick DT, Kolling GL, Fu Z, Guerrant RL (2016) Protein malnutrition impairs intestinal epithelial turnover: a potential mechanism of increased cryptosporidiosis in a murine model. Infect Immun 84(12):3542–3549. https://doi.org/10.1128/IAI.00705-16

Moawad HSF, Hegab MHAE, Badawey MSR, Ashoush SE, Ibrahim SM, Ali AAES (2021) Assessment of chitosan nanoparticles in improving the efficacy of nitazoxanide on cryptosporidiosis in immunosuppressed and immunocompetent murine models. J Parasit Dis 45(3):606–619. https://doi.org/10.1007/s12639-020-01337-y

Mohammed HS, Ibrahim MN, Zalat RS, Ahmed KA, Yaseen DI, Abdelhameed RM, Kishik SM (2021) Assessment of nitazoxanide loaded on silver nanoparticles efficacy on treatment of murine model of chronic toxoplasmosis. Benha Med J 38(1):186–199. https://doi.org/10.21608/bmfj.2021.144709

Oshiba SF, Ibrahim RY, Mohamed AE, Abdel Samie HA, El-Wakil EA (2018) In vivo effect of pomegranate (*Punica granatum*) extracts versus Nitazoxanide drug on the ileum of experimentally infected mice with *Cryptosporidium parvum* oocysts. J Am Sci 14(2):27–39

Ross MH, Pawlina W (2016) Histology: a text and atlas: with correlated cell and molecular biology, 7th edn. Wolters Kluwer, Philadelphia, p 984

Saad AA, Soliman MI, Azzam AM, Mostafa AB (2015) Antiparasitic activity of silver and copper oxide nanoparticles against *Entamoeba histolytica* and *Cryptosporidium parvum* cysts. J Egypt Soc Parasitol (JESP) 45(593–602):30–233. https://doi.org/10.1021/ml1002629

Said DE, El Samad LM, Gohar YM (2012) Validity of silver, chitosan and curcumin nanoparticles as *anti-Giardia* agents. Parasitol Res 111:545–554. https://doi.org/10.1007/s00436-012-2866-1

Samaka R, EL Shafei OK, Harba N, Farag S, Sharaf O (2021) Role of apoptosis in experimental *Cryptosporidium parvum* infected albino mice. J Egypt Soc Parasitol 51(1):89–98. https://doi.org/10.21608/JESP.2021.165944

Sasahara TH, Maruyama M, Aoki R, Kikuno T, Sekiguchi A, Takahashi Y, Satoh H, Kitasato Y, Takayama M, Inoue (2003) Apoptosis of intestinal crypt epithelium after *Cryptosporidium parvum* infection. J Infect Chemother 9:278–281. https://doi.org/10.1007/s10156-003-0259-1

Sedighi F, Abbasali Pourkabir R, Maghsood A, Fallah M (2016) Comparison of therapeutic effect of anti-*Cryptosporidium* nanonitazoxanide (NTZ) with free form of this drug in neonatal rat. Avicenna J Clin Med 23(2):134–140

Shaaban YM, Hassan ZR, Hassan AT, Hussein RR, Salama DEA (2021) Evaluation of the role of combined prebiotic and probiotic supplements as prophylactic and therapeutic agents against experimental giardiasis. PUJ 14(2):193–203. https://doi.org/10.21608/PUJ.2021.83828.1124

Sponseller JK, Grifths JK, Tzipori S (2014) The evolution of respiratory cryptosporidiosis: evidence for transmission by inhalation. Clin Microbiol Rev 27:575–586. https://doi.org/10.1128/CMR.00115-13

Taha MN, Salah A, Yousof HA, El-Sayed SH, Younis AI, Ismail MS (2017) Atorvastatin repurposing for the treatment of cryptosporidiosis in experimentally immunosuppressed mice. Exp Parasitol 181:57–69. https://doi.org/10.1016/j.exppara.2017.07.010

Uchiyama R, Tsutsui H (2015) Caspases as the key effectors of inflammatory responses against bacterial infection. Arch Immunol Ther Exp (Warsz) 63:1–13. https://doi.org/10.1007/s00005-014-0301-2

Wang C, Liu L, Zhu H, Zhang L, Wang R, Zhang Z, Huang J, Zhang S, Jian F, Ning C, Zhang L (2019) MicroRNA expression profile of HCT-8 cells in the early phase of *Cryptosporidium parvum* infection. BMC Genomics 20(1):37. https://doi.org/10.1186/s12864-018-5410-6

Xu Y, Tang H, Liu JH, Wang H, Liu Y (2013) Evaluation of the adjuvant effect of silver nanoparticles both in vitro and in vivo. Toxicol Lett 219:42–48. https://doi.org/10.1016/j.toxlet.2013.02.010

Zahir AA, Chauhan IS, Bagavan A, Kamaraj C, Elango G, Shankar J, Arjaria N, Roopan SM, Rahuman AA, Singh N (2015) Green synthesis of silver and Titanium Dioxide nanoparticles using *Euphorbia prostrata* extract shows shift from apoptosis to G0/G1 arrest followed by necrotic cell death in *Leishmania donovani*. Antimicrob Agents Chemother 59(8):4782–4799. https://doi.org/10.1128/AAC.00098-15